Molecular surveillance detects high prevalence of the neglected parasite *Mansonella ozzardi* in the Colombian Amazon

Dahmer KJ[1], Palma-Cuero M[1,2], Ciuoderis K[2,3], Patiño C[3], Roitman S[4], Li Z[4], Sinha A[4], Hite JL[1], Bellido Cuellar O[5], Hernandez-Ortiz JP[2,3], Osorio JE[1,2], Christensen BM[1,2], Carlow CKS[4], Zamanian M[1,2*]

[1] Department of Pathobiological Sciences, University of Wisconsin-Madison, Madison, WI USA
[2] University of Wisconsin Global Health Institute One Health Colombia, Madison, WI USA
[3] Universidad Nacional de Colombia - UW-GHI One Health Colombia, Medellín, Colombia
[4] New England Biolabs, 240 County Road, Ipswich, MA USA
[5] Secretaría de Salud Departamental del Amazonas, Leticia, Colombia

Correspondence: *mzamanian@wisc.edu

Abstract

Mansonellosis is an undermapped insect-transmitted disease caused by filarial nematodes that are estimated to infect hundreds of millions of people globally. Despite their prevalence, there are many outstanding questions regarding the general biology and health impacts of the responsible parasites. Historical reports suggest that the Colombian Amazon is endemic for mansonellosis and may serve as an ideal location to pursue these questions in the backdrop of other endemic and emerging pathogens. We deployed molecular and classical diagnostic approaches to survey *Mansonella* prevalence among adults belonging to indigenous communities along the Amazon River and its tributaries near Leticia, Colombia. Deployment of a loop-mediated isothermal amplification (LAMP) assay on blood samples revealed an infection prevalence of ~40% for *Mansonella ozzardi*. This assay identified significantly more infections than blood smear microscopy or LAMP assays performed using plasma, likely reflecting greater sensitivity and the ability to detect low microfilaremias or occult infections. *Mansonella* infection rates increased with age and were higher among males compared to females. Genomic analysis confirmed the presence of *M. ozzardi* that clusters closely with strains sequenced in neighboring countries. We successfully cryopreserved and revitalized *M. ozzardi* microfilariae, advancing the prospects of rearing infective larvae in controlled settings. These data suggest an underestimation of true mansonellosis prevalence, and we expect that these methods will help facilitate the study of mansonellosis in endemic and laboratory settings.

Keywords: *Mansonella ozzardi*, epidemiology, loop-mediated isothermal amplification, diagnostics, genomics, cryopreservation
Topic: Colombia, Amazonia, *Mansonella*, infection, infectious disease, *Culicoides*
Section: Parasitology

Introduction

Mansonellosis is a highly prevalent but undermapped [1] and understudied parasitic disease that infects hundreds of millions of people throughout Africa and Central and South America [2]. Three species of insect-transmitted parasitic nematodes (*Mansonella ozzardi, M. perstans* and *M. streptocerca*) are responsible for the majority of human cases although other *Mansonella* species have the potential to infect humans, including the recently discovered *Mansonella* sp. "DEUX" which has revitalized demands for allocating resources to study this severely neglected disease [2–5].

There are major gaps in our understanding of the basic biology and clinical or subclinical impacts of mansonellosis in human populations. *Mansonella* infections underlie variable clinical presentations that are likely underrecognized [4] and may alter host immunity in ways that alter vaccine responses and susceptibility to other pathogens [6–8]. Drugs used in mass drug administration campaigns for lymphatic filariasis and onchocerciasis are not as effective against *Mansonella spp.* [9–13] suggesting a unique genetic basis for anthelmintic resistance [14–16]. Additionally, *Mansonella* infections can introduce diagnostic challenges related to species mis-identification [17,18], cross-reactivity of immunochromatographic tests [19,20], and the inability to easily discern occult or amicrofilaremic infections [21]. Together, these limitations can potentially confound parasite elimination and surveillance programs focused on more prominent filarial worm parasites in co-endemic regions [9–13,16].

To address these challenges, we deployed both classical and molecular diagnostic approaches to carry out more precise epidemiological surveys of *Mansonella* prevalence in adults from villages along the Amazon River and its tributaries around the capital city of Leticia in the Amazonas Department of Colombia. The Amazon basin is historically associated with "new world" *M. ozzardi* [22–25] and is ideally situated to pursue fundamental questions about *Mansonella* biology, clinical presentations, and interactions with other pathogens that are endemic in the region. Parasite surveys in this region are outdated [22–24], but incidental findings from community health workers in the course of malaria screening and estimates from communities in neighboring countries [4,21,26] suggest a high prevalence.

The gold standard diagnostic for *M. perstans* and *M. ozzardi* is blood smear microscopy, which requires morphological differentiation of the circulating microfilariae (mf) stage [4,17]. Molecular diagnostic approaches including real-time PCR (RT-PCR) [27–29] are largely restricted to laboratory settings. However, more recently developed loop-mediated isothermal amplification (LAMP) assays with a simple colorimetric readout are more amenable to field studies [30]. We comparatively profiled LAMP assays with classical microscopy-based techniques to evaluate potential underestimation of parasite prevalence among a cluster of indigenous communities in the Colombian Amazon region. Microfilariae were isolated for population genomic analyses of *Mansonella* with respect to previously characterized field isolates, as well as for the establishment of a cryopreservation protocol to enable laboratory studies. Lastly, we probed associations of *Mansonella* infection status with other clinical and demographic variables. We expect that these data and methods will help facilitate future studies of *Mansonella*.

Methods

Study design and sampling procedure

This study was conducted between 2021 and 2023 in the Amazonas Department of Colombia in areas surrounding the capital city of Leticia and Puerto Nariño municipalities (**Figure 1A**). This region of vast biodiversity is largely populated by indigenous communities situated near the Amazon River and its tributaries. The study protocol was reviewed and approved by the UW-Madison IRB (study # 2019-1107) and Corporación para Investigaciones Biológicas (CIB #17022021). The study population (n = 235) from 13 communities was recruited by convenience and individuals ≥18 years of age were invited to participate and enrolled after providing written informed consent. Peripheral (venous) blood samples were collected into ethylenediaminetetraacetic acid (EDTA) tubes and thin and thick blood smears were prepared and examined for the presence of filarial parasites and malaria. Serum/plasma were extracted and aliquoted along with whole blood into 1.5 mL tubes and stored at -80°C for detection of *Mansonella* and other pathogens (**Figure 1B**). Self-reported socio-demographic and epidemiological data were collected using a structured questionnaire through face-to-face interviews at the enrollment site. Recorded data included demographics (age, sex, ethnicity, occupation, place of residence), housing conditions, travel history, medical history (pre-existing diseases), and clinical symptoms.

Figure 1
A) Map of the study region in the Amazonas Department of Colombia depicting the capital city of Leticia and the Puerto Nariño municipality where samples were collected across three surveys. The study region is adjacent to the Amazon River at the borders of Colombia, Brazil, and Peru. **B)** Schematic of sampling efforts and endpoints for blood samples acquired from adult volunteers. Blood smears and preparations of cryopreserved samples were conducted in the field. Whole blood was obtained in EDTA tubes and transferred on ice to a laboratory in Leticia. Aliquots of whole-blood and plasma were prepared from samples and used for downstream serology, molecular diagnostics, and genomic analyses. Questionnaires were filled out at the time of sampling.

Microscopy smears and microfilariae quantification

Routine thin and thick smears were prepared at the time of blood draws. Slides were allowed to dry at room temperature, Giemsa stained and examined microscopically. For quantitative microscopy, 40 µL of thawed blood was mixed with equal amounts of water and microfilaria (mf) were counted using light microscopy. For filtration of thawed blood aliquots, 1 mL of blood mixed with 4 ml of phosphate-buffered saline (PBS) was added to a Millipore syringe (Sigma-Aldrich, Z268429) with a 5 µm filter membrane (Millipore Sigma, TMTP02500). Filter membranes were imprinted in a microscope slide, allowed to dry before methanol fixation and Giemsa staining for microscopical observation.

Cryopreservation and recovery of microfilariae

Blood samples were transported on ice from Puerto Nariño to Leticia, where they were mixed with 5% dimethyl sulfoxide (DMSO) at a 1:1 ratio, aliquoted in cryogenic tubes and stored at -80°C [31]. Processed samples were then shipped to Medellin and stored at -80°C. Samples were thawed in a water bath at 37°C for 5 minutes and washed twice with sterile PBS (at 37°C), followed by centrifugation at 2,000 rpm for 10 minutes. The mf pellet was gently mixed with 2 mL of RPMI-1640 + 1x Antibiotic-Antimycotic (Gibco, 15240096). 1 mL aliquots were added to wells in a 6-well cell culture plate and the plate was incubated at 37°C and 5% CO_2. Movement patterns of mf were recorded using an inverted microscope (40X objective). Movement levels were quantified using a customized optical flow pipeline[32].

DNA extraction from blood and plasma samples

DNA was extracted from whole blood and plasma using the Quick-DNA 96-plus kit (Zymo, D4070/71) with minor adjustments to the protocol. For blood samples, the “solid tissue protocol” was followed by adding 50 µL of blood in place of water and tissue. After incubation for 2.5 hours, samples were spun at 3,500g for 2 minutes and supernatant lysate was transferred to the Zymo-spin 96-XL plate. For plasma samples, the “biological fluid and cells” protocol was followed. Final DNA was eluted with 15 µL of water and concentrations were assessed via NanoDrop for quality assurance.

Loop-mediated isothermal amplification assays

LAMP reactions were carried out as previously described [30] with slight modifications. Briefly, each LAMP reaction contained 1.6 µM each of primers FIP (5’-CGCAAACAGAAGCCCGAAAC-GCTCGCAATTTCATAGTGG-3’) and BIP (5’-CTTGCGCGTAGCATTAGATCC-TCCGAAATGTATACGACAGAT-3’), 0.2 µM each of F3 (5’-GCACGAAATGTTTTTGTACG-3’) and B3 (5’-CGTATCACCGTTGATGACG-3’), 0.4 µM each of LF (5’-AAGCCTAAGCCTAAGCCTGA-3’) and LB (5’-GCACATCTTCAATCTCCTCTTGC-3’), 2 µl 10X GuHCL, 10 µl of WarmStart Colorimetric LAMP 2x Master Mix (NEB, M1804L), 4 µl water and 2 µl of template DNA, or 2 µl water for non-template controls for a total volume of 20 µl per reaction. For a colorimetric readout, reactions were incubated at 63°C for 30 minutes in a SimpliAmp Thermocycler (Applied Biosystems, A24811) and images were acquired using an ImageQuant 800 (Cytiva). A post amplification color of yellow indicated detection of *M. ozzardi*, and pink (or orange) indicated no detection.

For semi-quantitative LAMP (sq-LAMP), simultaneous colorimetric and fluorescent readouts were obtained by adding SYTO™ 9 green (Invitrogen, S34854) to a final concentration of 1 µM in the colorimetric LAMP reaction. Reactions were performed in a Bio-Rad CFX Opus 96 Real-Time PCR instrument at 65°C with total fluorescence read in the SYBR/FAM channel every 15 seconds for 150 “cycles” (~53 minutes with each “cycle” corresponding to 21.2 seconds of reaction time, 15 seconds combined with plate reading time). A cut-off time threshold (Tt) value of 30 minutes was used to differentiate positive/negative reactions, with Tt defined as the time (min) to reach the fluorescence detection threshold. A Tt ≤ 30 minutes indicated the detection of

the target, whereas a Tt > 30 minutes or N/A, indicated no detection. Plates were scanned using the Epson Perfection v600 Photo Scanner.

DNA extraction and Illumina library construction and sequencing

DNA was extracted from 200 uL of whole blood using the MagAttract HMW DNA kit (Qiagen, 67563) following the manufacturer's instructions. The NEBNext Microbiome DNA enrichment kit (NEB, E2612) was used as directed to enrich *Mansonella* DNA and reduce human DNA prior to library construction. The Illumina libraries were constructed using the NEBNext Ultra II DNA Library Prep Kit for Illumina (NEB, E7645) as described by the manufacturer. The quality and concentration of each library were determined using a 2100 Bioanalyzer with a high-sensitivity DNA chip (Agilent Technologies). Libraries were diluted to 1 nM with 10 mM Tris, 0.1 mM EDTA pH 8. Phi X DNA (5%) was added to balance base pair composition in these A:T rich filarial libraries prior to sequencing on a NovaSeq platform (paired end, 150 bps).

Bioinformatic analysis

Raw Illumina reads were processed to remove adapters and poor-quality reads using the BBTools package (https://jgi.doe.gov/data-and-tools/bbtools/). For each isolate, the reads were mapped to a combined reference sequence set comprising a *M. ozzardi* reference genome from Brazil [16], a reference mitogenome KX822021.1 [33] and the *Wolbachia w*Moz assembly GCF_020278625.1 [34] using bowtie2 [35]. Reads mapping to mitochondria were extracted from the bam alignment files using samtools [36] and assembled into circular mitochondrial genomes using GetOrganelle v1.7.7.0 [37]. The average nucleotide identity scores between pairs of all assembled mitogenomes and published mitogenomes, namely the accessions KX822021.1 and MN416134.1 for *M. ozzardi* [21,33] and MT361687.1 and MN432521.1 for *M. perstans* [21,38] were calculated using the OrthoANIu tool [39]. Multiple sequence alignments of all *M. ozzardi* and *M. perstans* mitogenomes were obtained using mafft v7.149b [40]. The phylogenetic tree based on this alignment was generated using the iqtree online server [41], which performs automatic best fit substitution model selection using ModelFinder [42]. Bootstrap support values were calculated based on ultrafast bootstrap [43] with 1000 replicates. The tree was annotated on the iTOL webserver [44].

Serological tests for viral infections

Serum samples were used for antibody detection against several pathogens. Anti-dengue immunoglobulin G (IgG) and IgM were detected using SD BIOLINE Dengue Duo rapid test (Abbott), following manufacturer's instructions. Anti-Human Immunodeficiency Virus (HIV), Hepatitis B Virus (HBV), and Hepatitis C Virus (HCV) as well as anti-IgM against Severe Acute Respiratory Syndrome Coronavirus 2 (SARS-COV-2) were detected by chemiluminescence immunoassay using the Architect I1000 system (Abbott), following manufacturer's instructions.

Data analysis

Self-reported data were recorded on printed surveys by study personnel and completed forms were entered into Microsoft Excel by double entry. Excel spreadsheets were used for data inspection, cleaning, and quality control before data analysis using R Studio software v4.2.2 (42). To examine sex- and age-based differences of *M. ozzardi* infections, we used a linear model (lm) to get the residuals and assess the normality of our data. We determined our data did not follow a normal distribution (Shapiro-Wilk test, male age: W = 0.93224, p-value = 0.0002649 , female age: W = 0.89475, p-value = 8.05e-09). Based on these results, we ran a non-parametric Wilcox rank sum test with a p-value < 0.05 considered statistically significant. Next, to examine differences between infection prevalence across demographic variables and analyses on reported symptoms and serology results, we used generalized linear models (GLMs) with binomial distributions and log link functions [45]. We conducted model selection analyses using the *aictab* function in the R package AICcmodavg [46]. We built candidate models starting with the full model with all combinations of main effects among relevant biological and methodological factors, while avoiding overfitting. We compared candidate models using Akaike's information criterion and **Δ**AIC (the difference in AIC values for the focal model and the model with the lowest AIC, i.e., the 'winning' model) [47]. We also calculated the Akaike weight (w), which further quantifies the probability that a model is the most appropriate model relative to the candidate models (**Supplementary Table 1**). **Δ**AIC less than two and a higher w generally indicates that a model has substantial support while a suite of best models with low weights (w ~ 0) indicates that no single variable plays a substantial role in mediating infection dynamics [47]. Using the *Anova* function in the R package car [48], we assessed significance of the effects using Wald χ□2 statistics for the winning model.

Supplementary Table 1. Model selection for prevalence of *M. ozzardi* across demographic variables. Variables include age, sex, education, ethnicity, and location. Global = focal model, m8 = winning model.

Protocol and data availability

All pipelines for statistical analysis and data visualization are available at https://github.com/zamanianlab/Mansonella-ms.

Raw read data used for assembly of mitogenomes of *M. ozzardi* isolates Moz-Col-195, Moz-Col-204, Moz-Col-220 and Moz-Col-239 are submitted under NCBI BioProject XYZ. The accession numbers of the assembled mitogenomes are XYZ, XYZ, XYZ, XYZ respectively. The mitogenomes of isolates Moz-Brazil-1 and Moz-Venz-1 were assembled from previously reported raw read datasets [16] available from NCBI BioProject PRJNA917722 and PRJNA917766 respectively. The corresponding GenBank accessions for these mitogenomes are XYZ for Moz-Brazil-1 and XYZ for Moz-Venz-1.

Results

Parasite Prevalence

To assess *Mansonella* prevalence within our study population, we deployed a species-specific loop-mediated isothermal amplification (LAMP) assay [30] and compared diagnostic results with microscopic examination of thin blood smears. Across the first survey (samples 1-117), blood LAMP results show a higher prevalence of *M. ozzardi* infections (54/115, 46.9%) than single thin smear microscopy (16/104, 15.3%) and LAMP carried out using DNA from matched plasma (31/115, 26.9%) (**Figure 2 A**)**.** Consensus blood LAMP results were derived from experiments involving DNA extractions from independent aliquots of blood as well as replicates of LAMP assays carried out in two laboratories using DNA from a single extraction (**Supplementary Figure 1 A**).

Treating the blood LAMP as the truth case, thin smear microscopy shows a 31% sensitivity and plasma LAMP shows a 50% sensitivity. For the 30 samples where blood LAMP was positive and microscopy was negative, lower time (Tt) which is indicative of more parasite material being present in semi-quantitative LAMP (sq-LAMP) were observed (**Supplementary Figure 1 B-C**)**.** We therefore hypothesized that the discrepancy between LAMP results and microscopy is likely associated with lower titers of microfilariae in venous blood leading to thin smear false negatives [49] or occult (amicrofilaremic) infections [21] that can only be detected using molecular methods. In both cases, we would expect the blood LAMP assay to display better sensitivity.

Subsequent surveys (samples 118-186; samples 187-244) were used to probe potential associations between microfilaremia and *Mansonella* diagnostic results by incorporating quantitative microscopy. Blood LAMP assays showed an *M. ozzardi* prevalence of 33% (40/120). Among the 14 samples which tested positive in microscopy, 13 also tested positive in LAMP. Plasma LAMP (16%) and thin smear microscopy detected a lower prevalence (12%), reflecting the pattern observed in the first survey (**Figure 2 B**). Quantitative microscopy detected mf in 23/122 samples (19%), ranging from 0-11 mf/blood spot (**Figure 2 C**). Samples with the highest mf titers were most likely to be positive across blood and plasma LAMP assays and thin smears, while samples with lower mf titers were more likely to be negative in blood smears and only detected in the blood LAMP assay (**Figure 2 D**). This lends support to the hypothesis that low mf titers is a driver of false negatives in both thin smears and plasma LAMP assays.

To explore whether occult infections could also be a factor contributing to the positive blood LAMP samples which had negative microscopy results, we re-sampled blood from six individuals that fit this pattern. A larger volume of blood (1 mL) was filtered to identify mf that could be circulating at titers not routinely detectable via thick and thin smear microscopy. All six samples were still microscopy negative, supporting the likelihood of occult infections. Whole blood LAMP was the most sensitive diagnostic test and identified a prevalence of 40% for *M. ozzardi* across all three surveys (**Table 1**).

Figure 2

A) Diagnostic results derived from survey one blood samples (1-117) for in-field microscopy smears (M), LAMP using DNA extracted from blood (L_b), and LAMP using matched DNA extracted from plasma (L_p). **B)** Diagnostic results derived from surveys two and three (samples 118-244) for in-field microscopy smears (M), LAMP using DNA extracted from blood (L_b), and LAMP using matched DNA extracted from plasma (L_p). **C)** Quantitative microscopy counts (qM) derived from surveys two and three blood samples (118-244). **D)** Quantitative microscopy counts of microfilariae stratified by L_b and L_p results and coloured by microscopy smear results. (NN = negative L_b and negative L_p, IN= inconclusive L_b and negative L_p, PN = positive L_b and negative L_p, PP = positive L_b and positive L_p, NP = negative L_b and positive L_p). Grey = negative for *M. ozzardi*; White = no result (A-C). LAMP assay data are specific to *M. ozzardi*.

Supplementary Figure 1

A) Diagnostic results derived from survey one blood samples (1-117) for four replicates of LAMP using DNA extracted from blood samples (L_b) across two laboratories. Grey = negative for *M. ozzardi*. White = no result. **B)** Diagnostic results derived from survey one blood samples (1-117) for semi-quantitative LAMP (Tt). ND = not detected **C)** Semi-quantitative LAMP Tt counts (minutes) stratified by L_b and L_p results and colored by thin smear results. Dashed lines indicate Tt cuttoffs (> 1, <30 minutes = positive sq_LAMP). (NN = negative L_b and negative L_p, PN = positive L_b and negative L_p, PP = positive L_b and positive L_p, NP = negative L_b and positive L_p). LAMP assay data are specific to *M. ozzardi*.

Table 1. Summary and comparison of *M. ozzardi* diagnostic results for the entire study population.

Population Demographics

The three surveys consisted of individuals who reside in thirteen different communities situated between -02°50'14.9496" north latitude and -03°52'39.1980" south latitude; and -069°44'10.7880" and -070°35'52.2240" west longitude (Figure3 A). A majority of our sampled population were centered in Puerto Nariño (n = 136) (Table 2), where the prevalence of *M. ozzardi* as determined by blood LAMP is 44%. The next largest sampled communities in our survey, 12 de Octubre (24%; n = 25) and San Pedro de Tipisca (14%; n = 21), had lower prevalence. There was a higher prevalence of *M. ozzardi* mf identified via blood LAMP in males (49%; n = 84; mean age = 40.1 years) compared to females (32%; n = 148; mean age = 34.7 years). The mean age of *M. ozzardi* positive individuals was higher than the mean age of negative individuals in females (Wilcox: p = 0.026) but not males (Wilcox: p = 0.07) (Figure 3 B). To further examine differences between infection prevalence across demographic variables, we assessed significance of the fixed effects using Wald χ^2 statistics and identified education and place of residence as drivers of prevalence (education binomial GLM: χ^2 = 16.2647, p = 0.01240, case origin GLM: χ^2 = 13.6850, p = 0.03336). However, given the limitation of the data we were unable to confirm significant differences within these groups due to unequal and small sample sizes amongst subsets.

Clinical histories were collected and additional serological tests were carried out for survey two and three samples (n = 117) (**Figure 3 C**) and compared across *M. ozzardi* blood LAMP positive and negative individuals (**Figure 3 D**). Symptoms and serology results that were differentially reported (abdominal pain, fever, joint pain, muscle pain, Hepatitis B antibodies, and Hepatitis C antibodies) between blood LAMP positive and negative individuals were examined further to determine if fixed effects or *M. ozzardi* infections were more likely to explain these data. We assessed significance of the fixed effects and blood LAMP results using Wald χ^2 statistics and determined that *M. ozzardi* infection status did not significantly correlate to reported symptoms or serology results. Fixed effects including sex and age were identified as potential drivers of some of the reported symptoms and serology results but unequal and small sample sizes amongst subsets of data limited our post-hoc analysis.

Figure 3

A) A map of the study region in the Amazonas Department of Colombia depicting the community where individual participants reside. Point size reflects the number of samples collected and color represents the prevalence of *M. ozzardi* infection for each community. **B**) *M. ozzardi* prevalence as determined by blood LAMP assay stratified by sex and age (95% CI) (left) and histogram of *M. ozzardi* prevalence distribution by age (right). F = female, M = male **C**) *M. ozzardi* infection status and reported symptoms and serological test results for survey two and three individuals (n = 120). Orange = positive, present; Grey = negative, not-present; white indicates missing data. **D**) Donut plots reflecting relative fractions of *M. ozzardi* L_b positive and L_b negative individuals who self-reported symptoms and lab confirmed serological test results.

Table 2. Summary of Demographic and diagnostic data**.** Data includes a subset of the total study population where all summarized demographic information was provided on the questionnaire. (Age in years).

Genomic Analysis

Whole genome sequencing was performed on 4 samples (ID numbers 195, 204, 220 and 239) which tested positive in the *M. ozzardi* specific blood LAMP assay. Only sample 239 had detectable microfilariae in the quantitative microscopy assay. While a mapping analysis of the sequencing data showed that over 94% of the reads were from the human host, 1 to 6 % of reads mapped to the reference *M. ozzardi* genome assembly and to the *Wolbachia w*Moz genome assembly, although at a low coverage (**Supplementary Figure 2**).

Sufficient read coverage was obtained for successful assembly of complete, circular mitogenomes for each isolate. The assembled mitogenomes displayed more than 99.6% sequence identity to each other and to previously reported *M. ozzardi* mitogenomes from Brazil [21,33], as well as to the newly assembled mitogenomes from isolates Moz-Brazil-1 and Moz-Venz-1 obtained from Brazil and Venezuela respectively [16]. A phylogenetic analysis of all *M. ozzardi* mitogenomes in conjunction with *M. perstans* mitogenomes from Brazil [21] and Cameroon [38] showed a distinct *M. ozzardi* clade with very short branch lengths between various isolates and a clear separation from the *M. perstans* clade (**Figure 4**). Together, these results confirm the presence of *M. ozzardi* infection in these individuals.

Figure 4

Maximum-likelihood tree based on whole-mitogenome alignments of various *M. ozzardi* and *M. perstans* isolates. Abbreviation Moz and Mpe and indicate *M. ozzardi* and *M. perstans* respectively. The GenBank accessions are indicated in parenthesis next to isolate names, followed by the country of origin in the second parenthesis. Blue colors mark the isolates sequenced in this study. The DNA substitution model HKY+F+I was found to be the best fit according to Bayesian Information Criteria in ModelFinder. Values of ultrafast bootstrap support calculated with 1000 replicates is shown for branches with value higher than 80.

Supplementary Figure 2

A) Sequencing read coverage from different *M. ozzardi* isolates on the reference nuclear contigs from Moz-Venz-1 genome assembly. **B)** Sequencing read coverage from different *M. ozzardi* isolates on the *Wolbachia w*Moz reference genome assembly.

Cryopreservation of Blood-Dwelling Parasite Stage

As a first step towards establishing the lifecycle of *M. ozzardi* in a laboratory environment, we sought to functionally cryopreserve microfilariae and observe viable and active worms after thawing samples. We collected peripheral blood from individuals who were positive for *M. ozzardi* via blood LAMP assay and thin smear microscopy in our initial survey. Blood samples were mixed with dimethyl sulfoxide (DMSO) and kept at -80°C. We observed revitalization of microfilariae upon thawing at 37°C, whereby motility increased over the first 24 hour incubation period before steadily declining (**Figure 5 A**). Videos showed viable and healthy microfilariae (**Figure 5 B**) that may allow for membrane feeding of lab colonies of *Culicoides* and the production of infective-stage larvae (L3) in a laboratory setting.

Figure 5

A) Motility of cryo-preserved *M. ozzardi* microfilariae over 48 hours as measured by an optical flow algorithm. **B)** Brightfield images and optical flowmaps of videos used for motility analysis of thawed cryopreserved *Mansonella* samples aligned with the timepoints in (A). Brighter regions of the flowmaps reflect areas where more parasite movement was detected.

Discussion

We conducted three seroprevalence surveys to better map the distribution of *Mansonella* infections among indigenous communities in the Amazon basin of Colombia. Blood smear microscopy identified microfilariae in 12.7% of sampled individuals, which falls within the range of historical studies in the region [23,24,50]. Blood LAMP assays detected *M. ozzardi* DNA in 40% of sampled individuals, in closer agreement with more recent PCR-based surveys in the Amazon region of neighboring countries [26,28,51,52]. Our survey data adds to the growing body of evidence that microscopy-based approaches can drastically underestimate the true prevalence of global mansonellosis [5,14,26–30,51–53].

Molecular diagnostic assays can be leveraged to capture a broader range of infection states, including low microfilaremias or afilaremic (occult) infections [21]. The recovery of complete mitogenomes confirms the presence of *M. ozzardi* DNA in blood samples that previous microscopy diagnostics could not detect, providing further confidence in LAMP diagnostic results. The distribution of *M. ozzardi* adults within the human body is not fully resolved [54], but it is presumed that they commonly take residence in subcutaneous tissues and possibly the serous cavities. These larger stages are the likely source of blood-detectable nucleic acids in molecular diagnostic assays. LAMP assays provide a sensitive, specific, and potentially cost-effective approach for the surveillance of filarial nematode infections in human and vector populations [30,55–57]. The development of direct LAMP assays [58] not reliant on DNA extraction will add to the convenience of this approach in endemic settings.

The establishment of a cryopreservation protocol can facilitate the eventual rearing of *M. ozzardi* in laboratory settings, including controlled blood-feeding of reanimated microfilariae to susceptible colonies of biting midges. In vitro phenotyping of *Mansonella* drug responses [59] can help resolve the genetic and molecular basis for observed differences in antifilarial drug susceptibility across species [9,10,12,13,15,60] and open avenues for the screening and discovery of new therapeutic leads for mansonellosis.

Mansonella is neglected even among neglected pathogens due to a lack of investment in studying its biology and potential health impacts [4,8,61]. More complete demographic and clinical data are needed to determine *M. ozzardi* pathogenicity and assess risk factors. Adult worms disperse somewhat randomly into various tissues and body cavities, the consequences of which can vary considerably across individuals but have historically been summarized as relatively non-pathogenic. Although there are growing clinical case reports suggesting appreciable pathogenicity [4], it is difficult to streamline causal associations with more subtle health impacts. The current established threshold for addressing human filariasis is a causal association with significant morbidity, including blindness and physical disfigurement. Investigation of subclinical or secondary impacts of infection would shift the threshold of potential human clinical concern in mansonellosis-endemic regions to the same threshold that often triggers action as it relates to subclinical nematode infections of livestock and companion animals. We expect that improved diagnostic tools, growing genomic resources, and methods to study *Mansonella* in laboratory settings will facilitate this goal.

Acknowledgements

The authors thank the communities, the Secretaria de Salud Departamental del Amazonas, Alcaldia de Puerto Nariño, E.S.E Hospital San Rafael de Puerto Nariño, and the Laboratorio Departamental de Salud Pública de Leticia for their contributions to this study. We sincerely thank Julian Rodriguez and Corporacion Corpotropica for their assistance and coordination of activities at the study sites. In addition, we would like to thank the staff of One Health lab and auxiliary personnel at all the study sites for their assistance. Thanks to the Abbott Pandemic Defense Coalition for the provision of laboratory testing kits.

Funding

KJD was supported by a UW-SciMed GRS Fellowship (scimedgrs.wisc.edu) and NIH Parasitology and Vector Biology Training grant number T32 AI007414 (NIH.gov). This work was supported by a seed grant from the University of Wisconsin-Madison Global Health Institute (GHI) to MZ. CKSC, ZL, AS and SR gratefully acknowledge funding and support from New England Biolabs.

Conflicts

CKSC, ZL, AS and SR are employed by New England Biolabs, a manufacturer and vendor of molecular biology reagents. This affiliation does not affect the authors' impartiality, adherence to journal standards and policies or availability of data. All other authors report no potential conflicts of interest.

References

1. Schluth CG, Standley CJ, Bansal S, Carlson CJ. Spatial parasitology and the unmapped human helminthiases. Parasitology. **2023**; :1–9.

2. Bélard S, Gehringer C. High Prevalence of Mansonella Species and Parasitic Coinfections in Gabon Calls for an End to the Neglect of Mansonella Research. J Infect Dis. **2021**; 223(2):187–188.

3. Mourembou G, Fenollar F, Lekana-Douki JB, et al. Mansonella, including a Potential New Species, as Common Parasites in Children in Gabon. PLoS Negl Trop Dis. **2015**; 9(10):e0004155.

4. Ta-Tang T-H, Crainey JL, Post RJ, Luz SL, Rubio JM. Mansonellosis: current perspectives. Res Rep Trop Med. **2018**; 9:9–24.

5. Sandri TL, Kreidenweiss A, Cavallo S, et al. Molecular Epidemiology of Mansonella Species in Gabon. J Infect Dis. **2021**; 223(2):287–296.

6. Stensgaard A-S, Vounatsou P, Onapa AW, et al. Ecological Drivers of Mansonella perstans Infection in Uganda and Patterns of Co-endemicity with Lymphatic Filariasis and Malaria. PLoS Negl Trop Dis. **2016**; 10(1):e0004319.

7. Phillips RO, Frimpong M, Sarfo FS, et al. Infection with Mansonella perstans Nematodes in Buruli Ulcer Patients, Ghana. Emerg Infect Dis. **2014**; 20(6):1000–1003.

8. Ritter M, Ndongmo WPC, Njouendou AJ, et al. Mansonella perstans microfilaremic individuals are characterized by enhanced type 2 helper T and regulatory T and B cell subsets and dampened systemic innate and adaptive immune responses. PLoS Negl Trop Dis. **2018**; 12(1):e0006184.

9. Bregani ER, Rovellini A, Mbaïdoum N, Magnini MG. Comparison of different anthelminthic drug regimens against Mansonella perstans filariasis. Trans R Soc Trop Med Hyg. **2006**; 100(5):458–463.

10. Van Hoegaerden M, Ivanoff B, Flocard F, Salle A, Chabaud B. The use of mebendazole in the treatment of filariases due to Loa loa and Mansonella perstans. Ann Trop Med Parasitol. **1987**; 81(3):275–282.

11. Simonsen PE, Onapa AW, Asio SM. Mansonella perstans filariasis in Africa. Acta Trop. **2011**; 120 Suppl 1:S109–20.

12. Gonzalez AA, Chadee DD, Rawlins SC. Ivermectin treatment of mansonellosis in Trinidad. West Indian Med J. **1999**; 48(4):231–234.

13. Simonsen PE, Fischer PU, Hoerauf A, Weil G. Manson's Tropical Diseases, 23rd Edition: The Filariases. Manson's Tropical Diseases. unknown; 2014. p. 737–765.

14. Ta-Tang T-H, Luz SLB, Merino FJ, et al. Atypical Mansonella ozzardi Microfilariae from an Endemic Area of Brazilian Amazonia. Am J Trop Med Hyg. **2016**; 95(3):629–632.

15. Coulibaly YI, Dembele B, Diallo AA, et al. A randomized trial of doxycycline for Mansonella perstans infection. N Engl J Med. **2009**; 361(15):1448–1458.

16. Sinha A, Li Z, Poole CB, et al. Genomes of the human filarial parasites Mansonella perstans and Mansonella ozzardi. Frontiers in Tropical Diseases [Internet]. 2023 [cited 2023 Apr 3]; 4. Available from: https://doi.org/10.3389/fitd.2023.1139343

17. Mathison BA, Couturier MR, Pritt BS. Diagnostic Identification and Differentiation of Microfilariae. J Clin Microbiol [Internet]. **2019**; 57(10). Available from: http://dx.doi.org/10.1128/JCM.00706-19

18. Crainey JL, Bessa Luz SL. Light Microscopic Detection of Mansonella ozzardi Parasitemias. Clin. Infect. Dis. 2019. p. 2156.

19. Coulibaly YI, Soumaoro L, Dembele B, Hodges M, Zhang Y. POTENTIAL CROSS REACTIVITY OF MANSONELLA PERSTANS WITH WUCHERERIA BANCROFTI BY FILARIASIS TEST STRIPS. AMERICAN JOURNAL OF TROPICAL MEDICINE AND HYGIENE. AMER SOC TROP MED & HYGIENE 8000 WESTPARK DR, STE 130, MCLEAN, VA 22101 USA; 2019. p. 160–160.

20. Wanji S, Amvongo-Adjia N, Koudou B, et al. Cross-Reactivity of Filariais ICT Cards in Areas of Contrasting Endemicity of Loa loa and Mansonella perstans in Cameroon: Implications for Shrinking of the Lymphatic Filariasis Map in the Central African Region. PLoS Negl Trop Dis. **2015**; 9(11):e0004184.

21. Crainey JL, Costa CHA, Oliveira Leles LF de, et al. Deep Sequencing Reveals Occult Mansonellosis Coinfections in Residents From the Brazilian Amazon Village of São Gabriel da Cachoeira. Clin Infect Dis. **2020**; 71(8):1990–1993.

22. Kozek WJ, Palma G, Valencia W, Montalvo C, Spain J. Filariasis in Colombia: prevalence of Mansonella ozzardi in the Departamento de Meta, Intendencia del Casanare, and Comisaría del Vichada. Am J Trop Med Hyg. **1984**; 33(1):70–72.

23. Lightner LK, Ewert A, Corredor A, Sabogal E. A parasitologic survey for Mansonella ozzardi in the Comisaría del Vaupés, Colombia. Am J Trop Med Hyg. **1980**; 29(1):42–45.

24. Kozek WJ, D'Alessandro A, Silva J, Navarette SN. Filariasis in Colombia: prevalence of

518 mansonellosis in the teenage and adult population of the Colombian bank of the Amazon,
519 Comisaria del Amazonas. Am J Trop Med Hyg. **1982**; 31(6):1131–1136.

520 25. Tidwell MA, Tidwell MA. Development of Mansonella ozzardi in Simulium amazonicum, S.
521 argentiscutum, and Culicoides insinuatus from Amazonas, Colombia. Am J Trop Med Hyg.
522 American Society of Tropical Medicine and Hygiene; **1982**; 31(6):1137–1141.

523 26. Calvopina M, Chiluisa-Guacho C, Toapanta A, Fonseca D, Villacres I. High Prevalence of
524 Mansonella ozzardi Infection in the Amazon Region, Ecuador. Emerg Infect Dis. **2019**;
525 25(11):2081–2083.

526 27. Jiménez M, González LM, Carranza C, et al. Detection and discrimination of Loa loa,
527 Mansonella perstans and Wuchereria bancrofti by PCR-RFLP and nested-PCR of
528 ribosomal DNA ITS1 region. Exp Parasitol. **2011**; 127(1):282–286.

529 28. Tang T-HT, López-Vélez R, Lanza M, Shelley AJ, Rubio JM, Luz SLB. Nested PCR to
530 detect and distinguish the sympatric filarial species Onchocerca volvulus, Mansonella
531 ozzardi and Mansonella perstans in the Amazon Region. Mem Inst Oswaldo Cruz. **2010**;
532 105(6):823–828.

533 29. Fischer P, Büttner DW, Bamuhiiga J, Williams SA. Detection of the filarial parasite
534 Mansonella streptocerca in skin biopsies by a nested polymerase chain reaction-based
535 assay. Am J Trop Med Hyg. **1998**; 58(6):816–820.

536 30. Poole CB, Sinha A, Ettwiller L, et al. In Silico Identification of Novel Biomarkers and
537 Development of New Rapid Diagnostic Tests for the Filarial Parasites Mansonella perstans
538 and Mansonella ozzardi. Sci Rep. **2019**; 9(1):10275.

539 31. Zinser EW, McTier TL, Kernell NS, Woods DJ. Cryogenic preservation of Dirofilaria immitis
540 microfilariae, reactivation and completion of the life-cycle in the mosquito and vertebrate
541 hosts. Parasit Vectors. **2021**; 14(1):367.

542 32. Wheeler NJ, Gallo KJ, Rehborg EJG, Ryan KT, Chan JD, Zamanian M. wrmXpress: A
543 modular package for high-throughput image analysis of parasitic and free-living worms.
544 PLoS Negl Trop Dis. **2022**; 16(11):e0010937.

545 33. Crainey JL, Marín MA, Silva TRR da, et al. Mansonella ozzardi mitogenome and
546 pseudogene characterisation provides new perspectives on filarial parasite systematics and
547 CO-1 barcoding. Sci Rep. **2018**; 8(1):6158.

548 34. Sinha A, Li Z, Poole CB, et al. Multiple lineages of nematode-Wolbachia symbiosis in
549 supergroup F and convergent loss of bacterioferritin in filarial Wolbachia. Genome Biology
550 and Evolution. 2023; :evad073. Available from: https://doi.org/10.1093/gbe/evad073

551 35. Langmead B, Salzberg SL. Fast gapped-read alignment with Bowtie 2. Nat Methods. **2012**;
552 9(4):357–359.

553 36. Danecek P, Bonfield JK, Liddle J, et al. Twelve years of SAMtools and BCFtools.
554 Gigascience [Internet]. **2021**; 10(2). Available from:
555 http://dx.doi.org/10.1093/gigascience/giab008

556 37. Jin J-J, Yu W-B, Yang J-B, et al. GetOrganelle: a fast and versatile toolkit for accurate de

novo assembly of organelle genomes. Genome Biol. **2020**; 21(1):241.

38. Chung M, Aluvathingal J, Bromley RE, et al. Complete Mitochondrial Genome Sequence of Mansonella perstans. Microbiol Resour Announc [Internet]. **2020**; 9(30). Available from: http://dx.doi.org/10.1128/MRA.00490-20

39. Yoon S-H, Ha S-M, Lim J, Kwon S, Chun J. A large-scale evaluation of algorithms to calculate average nucleotide identity. Antonie Van Leeuwenhoek. **2017**; 110(10):1281–1286.

40. Nakamura T, Yamada KD, Tomii K, Katoh K. Parallelization of MAFFT for large-scale multiple sequence alignments. Bioinformatics. **2018**; 34(14):2490–2492.

41. Trifinopoulos J, Nguyen L-T, Haeseler A von, Minh BQ. W-IQ-TREE: a fast online phylogenetic tool for maximum likelihood analysis. Nucleic Acids Res. **2016**; 44(W1):W232–5.

42. Kalyaanamoorthy S, Minh BQ, Wong TKF, Haeseler A von, Jermiin LS. ModelFinder: fast model selection for accurate phylogenetic estimates. Nat Methods. **2017**; 14(6):587–589.

43. Hoang DT, Chernomor O, Haeseler A von, Minh BQ, Vinh LS. UFBoot2: Improving the Ultrafast Bootstrap Approximation. Mol Biol Evol. **2018**; 35(2):518–522.

44. Letunic I, Bork P. Interactive Tree Of Life (iTOL) v5: an online tool for phylogenetic tree display and annotation. Nucleic Acids Res. **2021**; 49(W1):W293–W296.

45. Crawley MJ. The R Book. John Wiley & Sons; 2012.

46. Mazerolle MJ. AICcmodavg: Model selection and multimodel inference based on (Q)AIC(c) [Internet]. 2023. Available from: https://cran.r-project.org/package=AICcmodavg

47. Burnham KP, Anderson DR. Model Selection and Inference: A Practical Information-Theoretic Approach. Springer New York; 1998.

48. Fox J, Weisberg S. An R Companion to Applied Regression. SAGE Publications; 2018.

49. Mischlinger J, Manego RZ, Mombo-Ngoma G, et al. Diagnostic performance of capillary and venous blood samples in the detection of Loa loa and Mansonella perstans microfilaraemia using light microscopy. PLoS Negl Trop Dis. **2021**; 15(8):e0009623.

50. Shelley AJ. A preliminary survey of the prevalence of Mansonella ozzardi in some rural communities on the river Purus, state of Amazonas, Brazil. Ann Trop Med Parasitol. **1975**; 69(3):407–412.

51. Abrahim CMM, Py-Daniel V, Luz SLB, Fraiji NA, Stefani MMA. Detection of Mansonella ozzardi among blood donors from highly endemic interior cities of Amazonas state, northern Brazil. Transfusion . **2019**; 59(3):1044–1051.

52. Medeiros JF, Almeida TAP, Silva LBT, et al. A field trial of a PCR-based Mansonella ozzardi diagnosis assay detects high-levels of submicroscopic M. ozzardi infections in both venous blood samples and FTA card dried blood spots. Parasit Vectors. **2015**; 8:280.

53. Medeiros JF, Fontes G, Nascimento VL do, et al. Sensitivity of diagnostic methods for

Mansonella ozzardi microfilariae detection in the Brazilian Amazon Region. Mem Inst Oswaldo Cruz. **2018**; 113(3):173–177.

54. Lima NF, Veggiani Aybar CA, Dantur Juri MJ, Ferreira MU. Mansonella ozzardi: a neglected New World filarial nematode. Pathog Glob Health. **2016**; 110(3):97–107.

55. Amambo GN, Innocentia N, Abong RA, et al. Application of loop mediated isothermal amplification (LAMP) assays for the detection of Onchocerca volvulus, Loa loa and Mansonella perstans in humans and vectors. Frontiers in Tropical Diseases [Internet]. **2023**; 3. Available from: https://www.frontiersin.org/articles/10.3389/fitd.2022.1016176

56. Ta-Tang T-H, Berzosa P, Rubio JM, et al. Evaluation of LAMP for the diagnosis of Loa loa infection in dried blood spots compared to PCR-based assays and microscopy. Mem Inst Oswaldo Cruz. **2022**; 116:e210210.

57. Poole CB, Li Z, Alhassan A, et al. Colorimetric tests for diagnosis of filarial infection and vector surveillance using non-instrumented nucleic acid loop-mediated isothermal amplification (NINA-LAMP). PLoS One. **2017**; 12(2):e0169011.

58. Avendaño C, Patarroyo MA. Loop-Mediated Isothermal Amplification as Point-of-Care Diagnosis for Neglected Parasitic Infections. Int J Mol Sci [Internet]. **2020**; 21(21). Available from: http://dx.doi.org/10.3390/ijms21217981

59. Njouendou AJ, Kien CA, Esum ME, et al. In vitro maintenance of Mansonella perstans microfilariae and its relevance for drug screening. Exp Parasitol. **2019**; 206:107769.

60. Fischer P, Tukesiga E, Büttner DW. Long-term suppression of Mansonella streptocerca microfilariae after treatment with ivermectin. J Infect Dis. **1999**; 180(4):1403–1405.

61. Metenou S, Babu S, Nutman TB. Impact of filarial infections on coincident intracellular pathogens: Mycobacterium tuberculosis and Plasmodium falciparum. Curr Opin HIV AIDS. **2012**; 7(3):231–238.

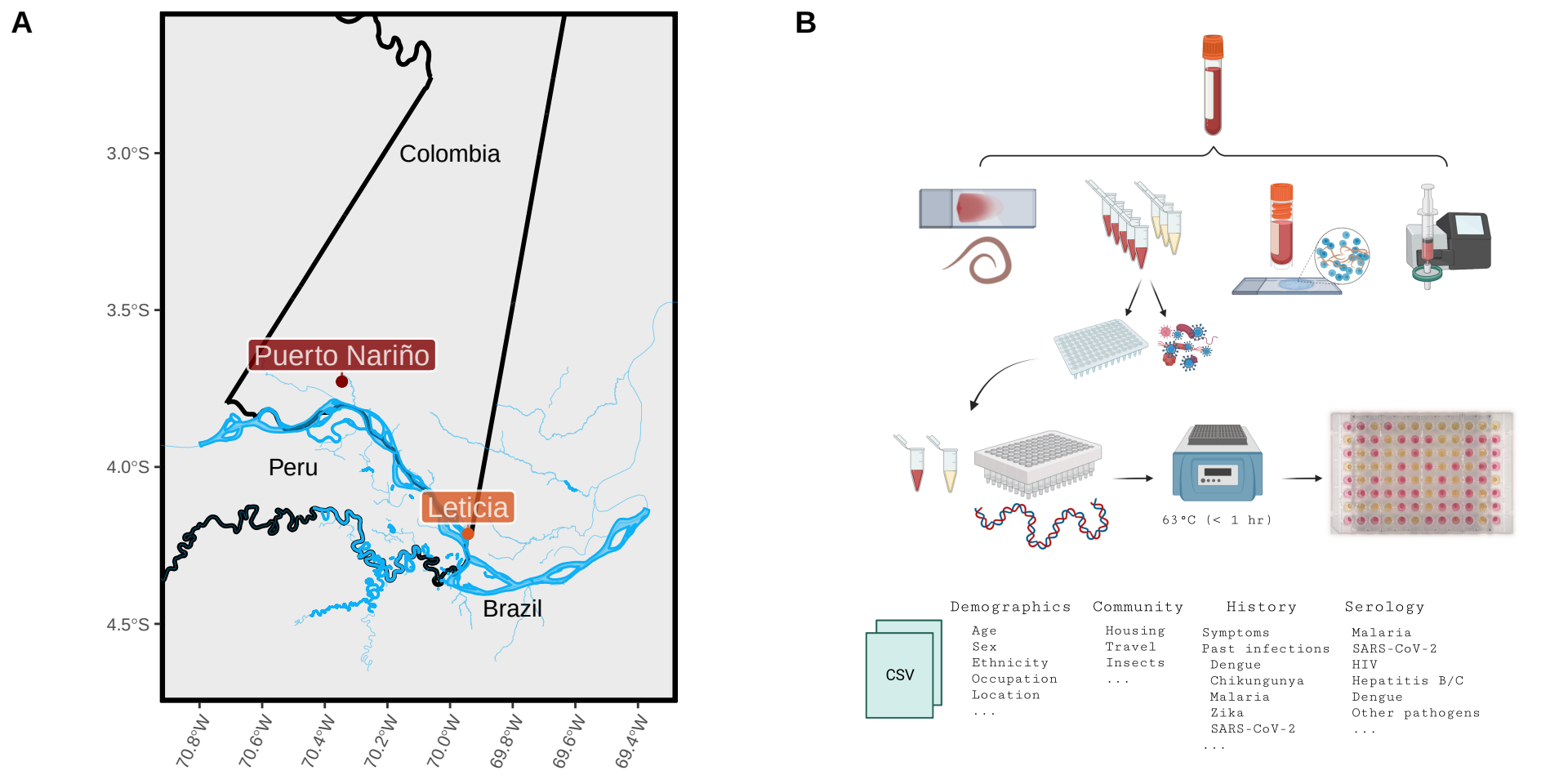
A
Colombia
Puerto Nariño
Peru
Leticia
Brazil
3.0°S
3.5°S
4.0°S
4.5°S
70.8°W
70.6°W
70.4°W
70.2°W
70.0°W
69.8°W
69.6°W
69.4°W
B
63°C (< 1 hr)
CSV
Demographics
Age
Sex
Ethnicity
Occupation
Location
...
Community
Housing
Travel
Insects
...
History
Symptoms
Past infections
Dengue
Chikungunya
Malaria
Zika
SARS-CoV-2
...
Serology
Malaria
SARS-CoV-2
HIV
Hepatitis B/C
Dengue
Other pathogens
...

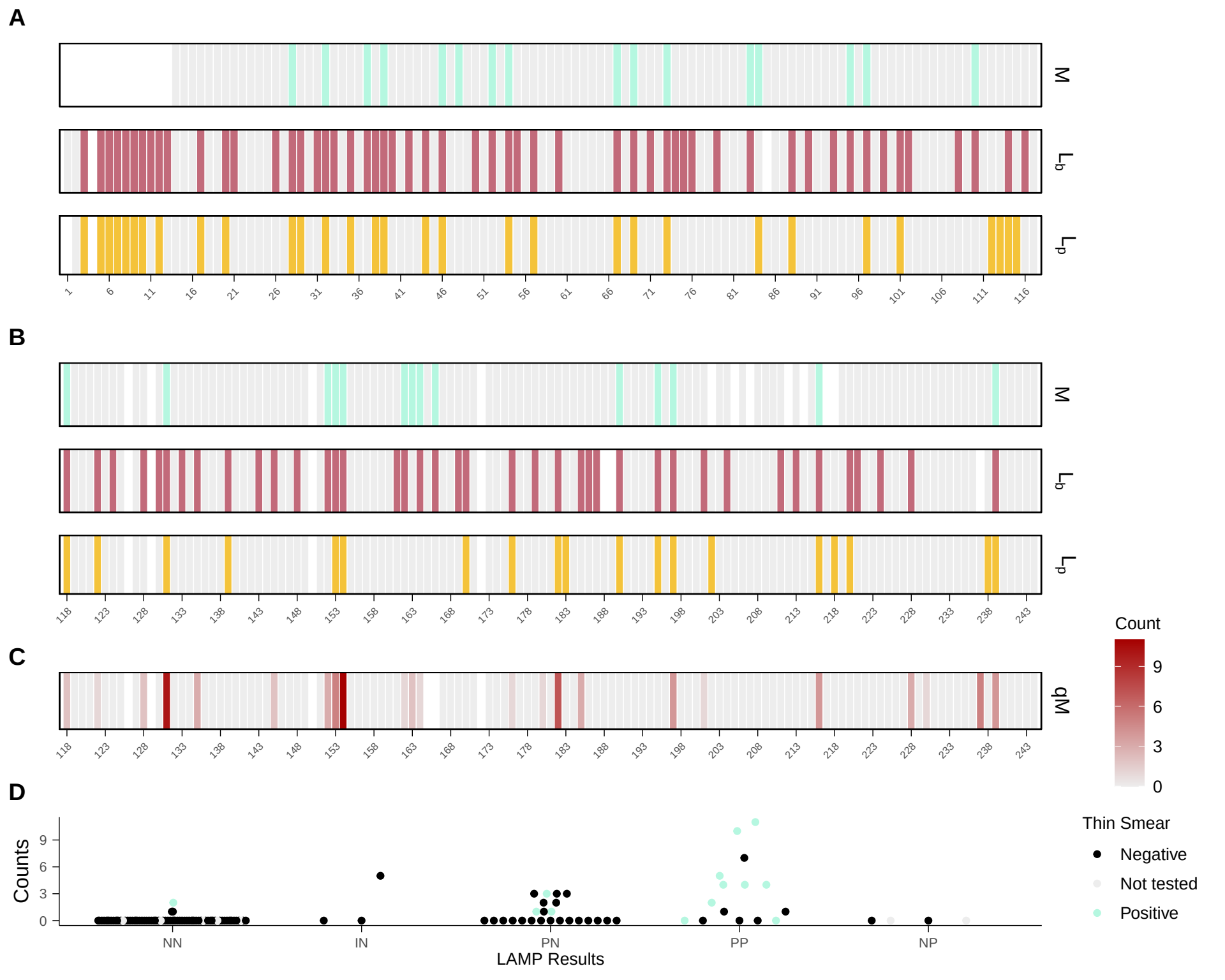
A
M
Lb
Lp
1 6 11 16 21 26 31 36 41 46 51 56 61 66 71 76 81 86 91 96 101 106 111 116
B
M
Lb
Lp
118 123 128 133 138 143 148 153 158 163 168 173 178 183 188 193 198 203 208 213 218 223 228 233 238 243
C
qM
118 123 128 133 138 143 148 153 158 163 168 173 178 183 188 193 198 203 208 213 218 223 228 233 238 243
Count
9
6
3
0
D
Counts
9
6
3
0
NN
IN
PN
PP
NP
LAMP Results
Thin Smear
Negative
Not tested
Positive

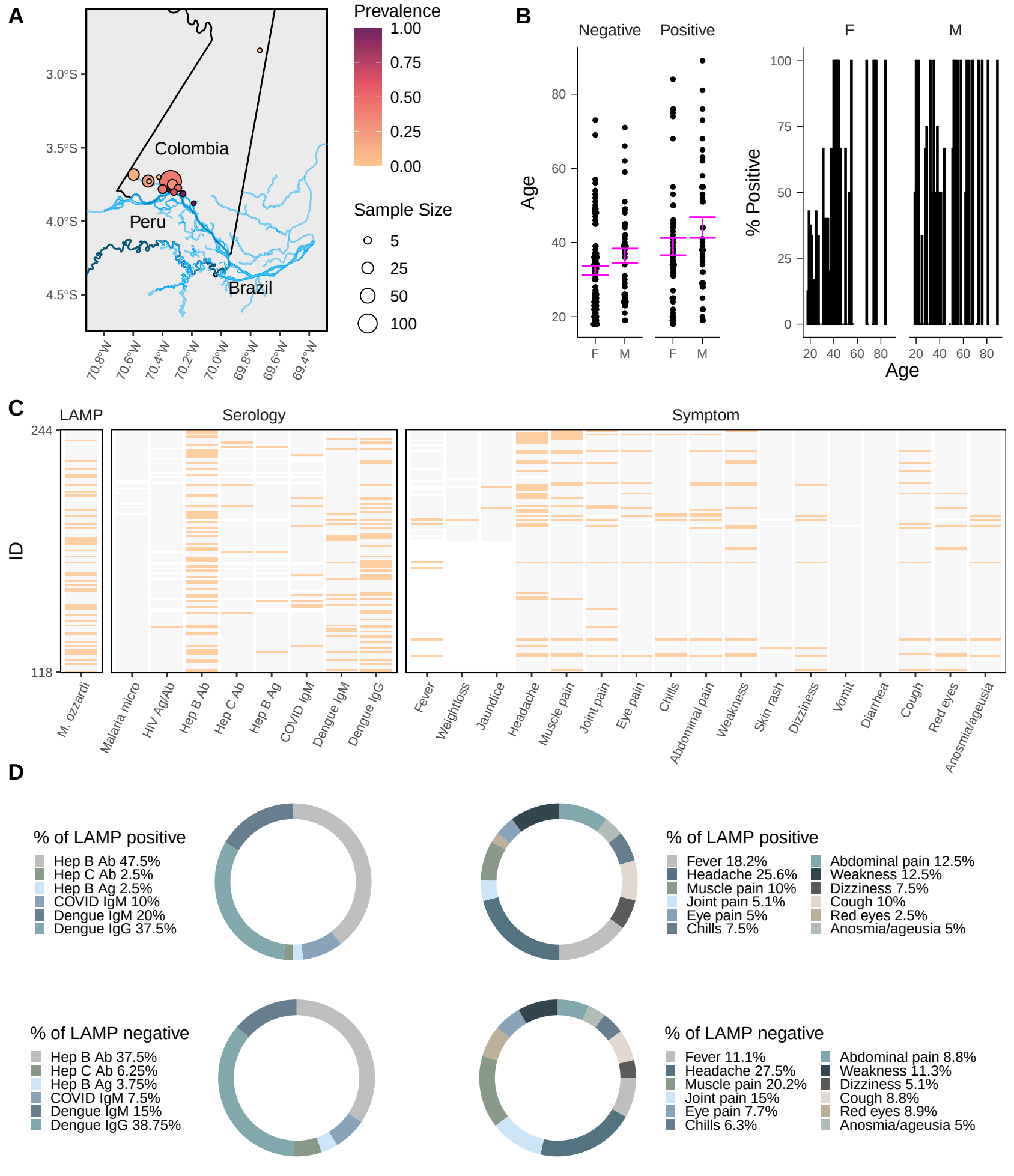
A
Prevalence
1.00
0.75
0.50
0.25
0.00
Sample Size
5
25
50
100
Colombia
Peru
Brazil
3.0°S
3.5°S
4.0°S
4.5°S
70.8°W
70.6°W
70.4°W
70.2°W
70.0°W
69.8°W
69.6°W
69.4°W
B
Negative
Positive
F
M
Age
% Positive
C
LAMP
Serology
Symptom
ID
244
118
M. ozzardi
Malaria micro
HIV Ag/Ab
Hep B Ab
Hep C Ab
Hep B Ag
COVID IgM
Dengue IgM
Dengue IgG
Fever
Weightloss
Jaundice
Headache
Muscle pain
Joint pain
Eye pain
Chills
Abdominal pain
Weakness
Skin rash
Dizziness
Vomit
Diarrhea
Cough
Red eyes
Anosmia/ageusia
D
% of LAMP positive
Hep B Ab 47.5%
Hep C Ab 2.5%
Hep B Ag 2.5%
COVID IgM 10%
Dengue IgM 20%
Dengue IgG 37.5%
% of LAMP positive
Fever 18.2%
Headache 25.6%
Muscle pain 10%
Joint pain 5.1%
Eye pain 5%
Chills 7.5%
Abdominal pain 12.5%
Weakness 12.5%
Dizziness 7.5%
Cough 10%
Red eyes 2.5%
Anosmia/ageusia 5%
% of LAMP negative
Hep B Ab 37.5%
Hep C Ab 6.25%
Hep B Ag 3.75%
COVID IgM 7.5%
Dengue IgM 15%
Dengue IgG 38.75%
% of LAMP negative
Fever 11.1%
Headache 27.5%
Muscle pain 20.2%
Joint pain 15%
Eye pain 7.7%
Chills 6.3%
Abdominal pain 8.8%
Weakness 11.3%
Dizziness 5.1%
Cough 8.8%
Red eyes 8.9%
Anosmia/ageusia 5%

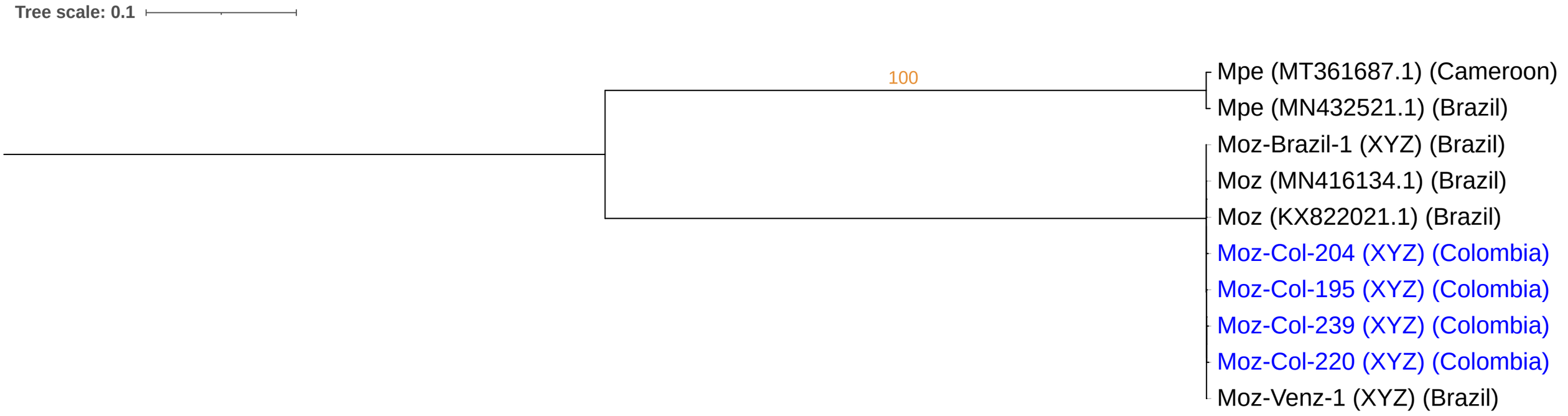
Tree scale: 0.1
100
Mpe (MT361687.1) (Cameroon)
Mpe (MN432521.1) (Brazil)
Moz-Brazil-1 (XYZ) (Brazil)
Moz (MN416134.1) (Brazil)
Moz (KX822021.1) (Brazil)
Moz-Col-204 (XYZ) (Colombia)
Moz-Col-195 (XYZ) (Colombia)
Moz-Col-239 (XYZ) (Colombia)
Moz-Col-220 (XYZ) (Colombia)
Moz-Venz-1 (XYZ) (Brazil)

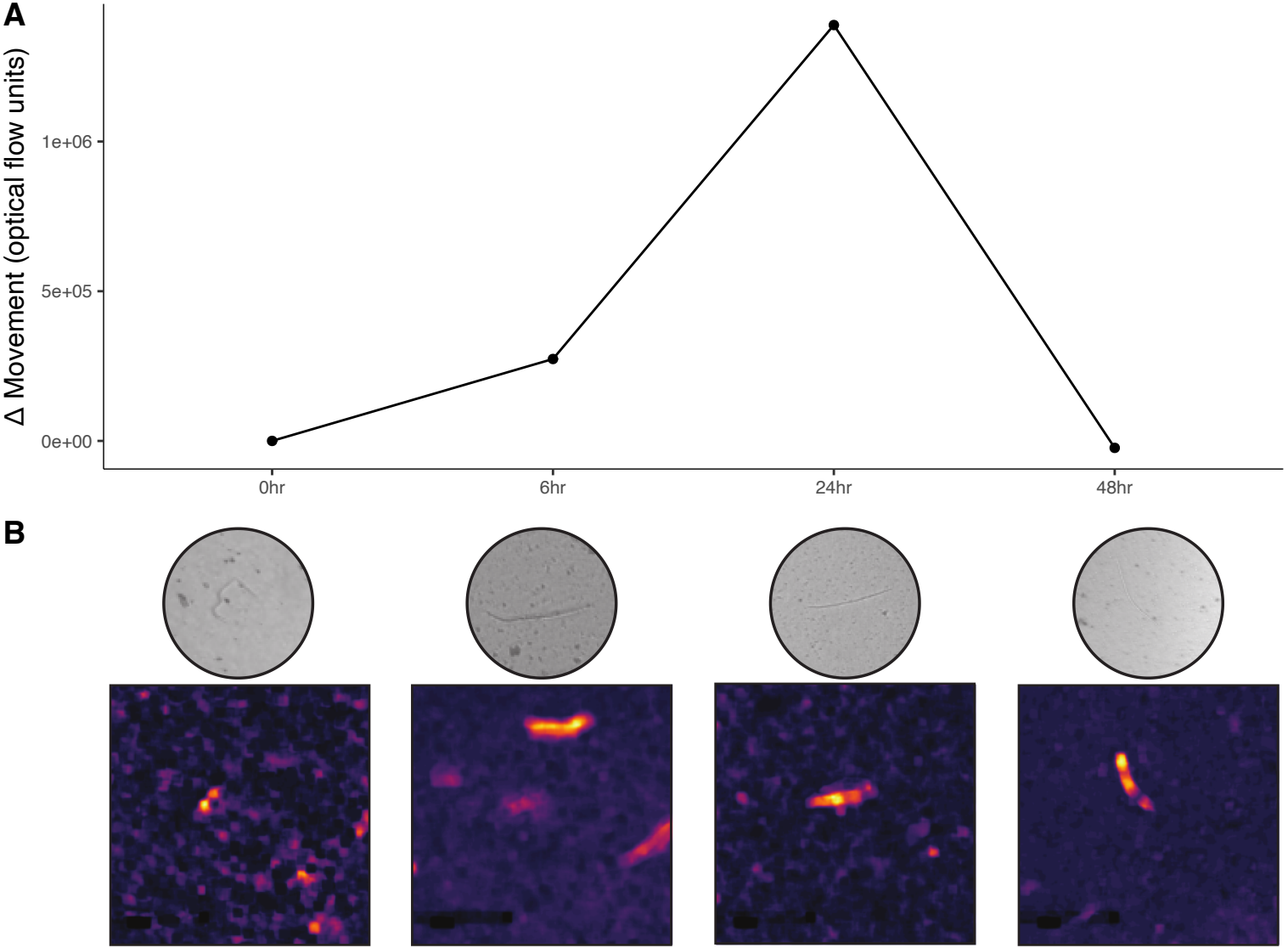
A
Δ Movement (optical flow units)
1e+06
5e+05
0e+00
0hr
6hr
24hr
48hr
B

	Microscopy Smear / LAMP-Plasma Positive	Microscopy Smear / LAMP-Plasma Negative	No Result	Total
LAMP-Blood Positive	27 / 42	57 / 52	10 / 0	94
LAMP-Blood Negative	3 / 8	129 / 132	9 / 1	141
	30 / 50	186 / 184	19 / 1	235

	Young Adult 18 - 32	Adult 33 - 54	Mature Adult 55 - 89	Total				
Age	101	104	29	234				
Sex (Female / Male)	69 / 32	68 / 36	12 / 17	149 / 85				
M. ozzardi (L_b / L_p / Microscopy)	31 / 16 / 9	42 / 24 / 16	20 / 10 / 5	93 / 50 / 30				
	Primary	High School	Technical	University	Other	Not Reported		
Education	59	81	52	16	2	24		
	Bora	Cocama	Senu	Ticuna	Tokami	Multiethnic	Not Reported	
Ethnicity	1	5	1	151	1	3	72	
	Lomas Lindas	12 De Octubre	San Francisco	Villa Andrea	Puerto Narino	San Pedro De Tipisca	Other	Not Reported
Location	11	25	9	15	136	21	14	3